

# Mathematical modelling for collective chemotaxis and aerotaxis response of *Escherichia coli*

R.V.S. Uday bhaskar\* Mahesh S. Tirumkudulu\*\*  
Kareenhalli V. Venkatesh\*\*\*

\* Department of Chemical Engineering, Indian Institute of Technology, Mumbai, India 400076 (e-mail: rvsbhaskar2001@che.iitb.ac.in)

\*\* Department of Chemical Engineering, Indian Institute of Technology, Mumbai, India 400076 (e-mail: mahesh@che.iitb.ac.in)

\*\*\* Department of Chemical Engineering, Indian Institute of Technology, Mumbai, India 400076 (e-mail: venks@iitb.ac.in)

---

**Abstract:** The phenomenon by which *Escherichia coli* (*E. coli*) move towards or away from a chemical by altering its swimming pattern is termed as Chemotaxis. The binding of ligands to trans-membrane receptors present on the cell surface results in a series of intra-cellular reactions that ultimately controls the bias of the flagella motors and in turn alters the swimming pattern. A similar phenotypic response has been observed in gradients of oxygen, termed as aerotaxis, though the intra-cellular pathway responsible for the effect is not understood. In this paper, we propose a simple model based on a generic adaptation mechanism that captures the cell's response to a time varying concentration of oxygen. Our model incorporates both the mechanisms of aerotaxis and chemotaxis and predicts the motion of a cell in a gradient of Methyl Aspartate. The predictions are in good agreement with the measurements of drift velocity in controlled gradients of Methyl Aspartate.

*Keywords:* Chemotaxis, Aerotaxis, Diffusion, *Escherichia coli*, Adaptation

---

## 1. INTRODUCTION

Chemotaxis is the migratory response of cells in the presence of a chemical. Chemicals to which cells respond are called chemotactants. A cell moves in the direction of increasing chemical gradient for a chemoattractant while it moves in the opposite direction in case of chemorepellents. Examples of chemoattractants for *Escherichia coli* (*E. coli*) are sugars, amino acids, peptides etc., while the chemorepellents include antibiotics, metal ions, toxic chemicals etc. Chemotaxis has been extensively studied in *Escherichia coli* (*E. coli*) (Eisenbach, 2004). The *E. coli* generates thrust (and therefore runs) via flagella which bundle when they rotate in the counter clockwise (CCW) direction while clockwise rotation of one or more of the flagellum unbundles the flagella to give a new random direction called a tumble. *E. coli* modulates its run and tumble motion so as to direct its net movement towards favorable environment. The regulation of the motor bias is achieved through a well characterized signaling pathway which involves sensing of the ligand through a membrane sensor, response through a signaling pathway and adaptation to the new environments. The regulation of chemotaxis involves CheW protein that couples a kinase, CheA, to methyl-accepting chemotaxis proteins (MCPs) to form a complex. In this mechanism, CheA autophosphorylates which in phosphorylates a regulator protein, CheY to CheY-P. The latter interacts with a flagellar motor switch protein FliM causing the motor to run clockwise

leading to a tumble. When a ligand (attractant) binds to the receptor, the rate of autophosphorylation of CheA decreases causing dephosphorylation of CheY-P thereby reducing the tumbling frequency and allowing the cell to run smoothly in the favorable environment. CheA phosphorylation is returned to its original level via a feedback mechanism involving methylation and demethylation of the receptor which in turn returns the CW bias to the pre-stimulus level. This mechanism allows the cell to adapt to a new environment through a transient where the CW bias alone is modulated (Eisenbach, 2004).

*E. coli* has five distinct chemotaxis receptors, namely, Tar, Tsr, Trg, Tap and Aer. While the existing knowledge of the signaling pathway is essentially based on studies involving Tar in response to non-metabolizable amino acid,  $\alpha$ -methyl-DL-aspartate (MeAsp), it is only recently that the intra-cellular mechanism of aerotaxis, where the cell moves in response to varying oxygen concentration, is becoming clear. *E. coli* senses oxygen via the Aer receptor which has a MCP-like signaling domain but lacks the sensing domain. Aer has Flavin Adenine Dinucleotide (FAD) binding Per Arnt Sim (PAS) domain in the cytoplasm, joined to a membrane anchor by a F1 linker (Laszlo and Taylor, 1981). The PAS domain senses the changes in extracellular oxygen by detecting the redox changes in the cell through cytosolic electron donors like NADH or by direct interaction with electron transport system. The signals corresponding to the measured changes in the level of oxygen converge in the chemotactic signaling pathway

at the CheA histidine kinase system (Rebbapragada et al., 1997).

Experiments, such as those by Vuppula et al. (2010), have quantified the contribution of oxygen to the overall response of a cell in the presence of steady gradients of a chemotactant. Here, a concentrated pellet of cells was introduced at one end of a horizontal capillary tube containing a linear gradient of MeAsp. The cells emerge from the pellet and move up gradient of the ligand. The measured drift velocity in response to a fixed gradient of MeAsp varied with the level of initial oxygen concentration in the media indicating that the cells simultaneously consume oxygen and respond to the resulting oxygen gradients. Further Vuppula et al. (2010) show that the net drift velocity can be obtained by adding the response to the MeAsp gradient and that due to the oxygen gradient.

In this paper, we propose a simple model that combines the existing two state model (Barkai and Leibler (1997)) involving the Tar receptor along with a simple phenomenological model based on a generic adaptation mechanism (Inoue and Kaneko (2006)) that captures the cell's response to a time varying concentration of both MeAsp and oxygen. The model predictions compare well with the measured time varying motor bias to a step change in oxygen concentration. For fixed gradients of Methyl Aspartate, we solve for the spatial variation of oxygen concentration via the convection-diffusion equation that includes a consumption term. The predicted drift velocity is high initially and decreases as the cells move up the gradient. This trend matches with the measurements though the predicted predicted velocities are some what lower.

## 2. MODEL DEVELOPMENT

*E. coli* response to ligand comprises of three modules, sensing of ligand by receptor, signal transmission by network of proteins and execution of response by flagella. Model equations that were used to describe these three modules are discussed below.

### 2.1 Sensing of ligand

Response of *E. coli* to a ligand in an aerobic environment comprises of aerotaxis and chemotaxis. Chemotaxis and aerotaxis are sensed independently by the receptors and transmit the signals to a common histidine kinase, *CheA*.

*Model equations for aerotaxis* Aer senses the presence of oxygen in the environment and send appropriate signal to histidine kinase. Experiments have also suggested a role of Tsr in aerotaxis. Here, we consider the combined effect of the sensing through a single aerotaxis receptor. A simple mathematical formulation present by Inoue and Kaneko (2006) is used to explain the dynamics of aerotaxis receptor. The aerotactic receptor is assumed to exist in two responsive states, namely, active and inactive, where the latter decrease the phosphorylation of CheA. Following Inoue and Kaneko (2006), we introduce a second variable,  $v$ , such that at its time evolution equation returns the state of the aerotaxis receptor ( $T^o$ ) at steady state to its pre-stimulus value. This ensures that the response due to aerotaxis always leads to a perfect adaptation. The

receptor activation is captured through a Hill function in terms of the oxygen concentration ( $C_{O_2}$ ) as given below,

$$\frac{dT^o}{dt} = \frac{kC_{O_2}^n}{k_O + C_{O_2}^n} - \beta v T^o - \alpha T^o \quad (1)$$

$$\frac{dv}{dt} = \beta v T^o - \gamma v \quad (2)$$

where  $k$ ,  $k_O$ ,  $\alpha$ ,  $\beta$ ,  $\gamma$  and  $n$  are the relevant parameters that represent the dynamics of the aerotactic receptors. Here  $T^o$  is not a conserved moiety, it is equivalent to  $T^A$  in case of chemotaxis.

*Model equations for chemotaxis* The two-state model proposed by Barkai and Leibler (1997) is used to describe the receptor dynamics for chemotaxis. Methylation and demethylation rates of receptors in the presence of CheR and CheB-p determines the dynamics of receptors. Chemotaxis receptor equations are explained in detail in the appendix A.

### 2.2 Signalling Trasduction

Signals in response to oxygen and MeAsp converge at CheA histidine kinase which is reflected in the additional term,  $k_1 T^o A$ , in equation 3. The first term captures the response to MeAsp via the Tar receptor and is consistent with the model of Barkai and Leibler (1997). Thus the active chemotaxis and aerotaxis receptors increase the phosphorylation rate of CheA. The phosphorylated CheA-p transfers its phosphate group to CheY and CheB. Recall that concentration of CheY-p decides the cell response by interacting with FlhM protein of flagella. Dynamics of CheA-p, CheB-p and CheY-p are given in equations 3 to 5, while the rate constants (other than  $k_1$ ) were taken from Vuppula et al. (2010).

$$\frac{dA_p}{dt} = 23.5(T^o A)A - 100(A_p)Y - 10(A_p)B - k_1 T^o A \quad (3)$$

$$\frac{dY_p}{dt} = 100(A_p)Y - 30(Y_p) \quad (4)$$

$$\frac{dB_p}{dt} = 10(A_p)B - (B_p) \quad (5)$$

Here,  $A$ ,  $A_p$ ,  $Y$ ,  $Y_p$ ,  $B$  and  $B_p$  represent, respectively, the concentrations of CheA, phosphorylated CheA, CheY, phosphorylated CheY, CheB and phosphorylated CheB. Li and Hazelbauer (2004) have measured these chemotaxis protein concentrations for wild type *E. coli* and are given by,  $A + A_p = 5.3 \mu\text{M}$ ,  $B + B_p = 0.28 \mu\text{M}$ ,  $Y + Y_p = 9.7 \mu\text{M}$  and CheR ( $R$ ) =  $0.16 \mu\text{M}$ . The total receptor concentration,  $T_0 + T_1 + T_2 + T_3 + T_4 = 17 \mu\text{M}$  and  $R = 0.16 \mu\text{M}$ . These values are identical to that used for sensing of MeAsp. The above equations were solved in conjunction with Tar receptor equations (appendix) to obtain the dynamics of the signaling network.

### 2.3 Motion of cell

The above intra-cellular pathway determines the concentration of CheY-p which in turn decides the CW bias of the cell, i.e., fraction of time cell spends in tumbling. Vuppula

et al. (2010) use a Hill relation to relate the CW bias and CheY-P ( $Y_p$ ) concentration with a Hill coefficient ( $n$ ) of 50 and a Half saturation constant ( $K$ ) of  $3.1 \mu\text{M}$ ,

$$CW = \frac{Y_p^n}{Y_p^n + K^n} \quad (6)$$

We use the same values in the simulations. The calculated CW bias was used to determine the time spent in the tumble and run mode. The time spent by the cell in the tumble mode ( $t_{tum}$ ) is the ratio of the CW bias to the switching frequency ( $F = \frac{dCW}{dY_p}$ ) while that in the run mode ( $t_{run}$ ) is the ratio of CCW bias to the switching frequency.

$$t_{tum} = \frac{CW}{F} \quad (7)$$

$$t_{run} = \frac{1 - CW}{F} \quad (8)$$

The probability that a cell in the run mode will tumble ( $P_{tum}$ ) is equal to the ratio of the discrete time step used in the simulation to the run time,

$$P_{tum} = \frac{dt}{t_{run}} \quad (9)$$

Similarly, the probability that a cell in the tumble mode will run ( $P_{run}$ ) is equal to the ratio of the discrete time step used in the simulation to the tumble time,

$$P_{run} = \frac{dt}{t_{tum}} \quad (10)$$

In our simulations, for a cell already in a run mode, we generate a random number between 0 and 1, and compare this value with the probability that the cell will tumble. If the generated random number is less than the probability value, then it will tumble else it will continue to run. A similar procedure is used to decide a run when the cell is in the tumble mode. Simulations were performed to capture the motion of *E. coli* in a capillary for a steady concentration gradient of MeAsp. Concentration of MeAsp in the capillary varies linearly with position ( $x$ ),  $L(x) = L_0 + Gx$ , where  $L_0$  is MeAsp concentration at  $x = 0$  and  $G$  is the gradient. *E. coli* moves in response to MeAsp gradient and consumes oxygen, thereby establishing an oxygen gradient. Therefore, the cell movement is determined by the combined response to MeAsp and oxygen. The oxygen concentration in the capillary is determined using a diffusion equation that also accounts for the consumption of oxygen by the bacteria,

$$\frac{\partial C_{O_2}}{\partial t} = D \frac{\partial^2 C_{O_2}}{\partial x^2} - N_{cell}(x)\theta(C_{O_2}) \quad (11)$$

Here,  $N_{cell}(x)$  is the cell density. Cell density is cell distribution in the capillary per unit volume of the capillary. It gets updated after every step in simulation using the cells distribution obtained. Distribution of cells in the capillary are divided into 5 equal bins. In each bin cell density, number of cells present in the bin divided by its volume is measured. While  $D = 2000 \mu\text{m}^2/\text{s}$  is the oxygen diffusivity (Cussler, 1997). To ensure that oxygen consumption by the cell decreases as oxygen concentration declines,  $\theta$  is assumed to follow Michaelis-Menten kinetics.

$$\theta(C_{O_2}) = c_r \frac{C_{O_2}}{C_{O_2} + k_0} \quad (12)$$

where  $c_r$  is the maximum oxygen consumption rate by *E. coli* i.e.,  $10^{-15}$  mg/s bacterium (Martin, 1932) and

$k_0$  is the Michaelis Menton constant. The capillary has initially a uniform concentration of oxygen ( $C_i$ ) while cells are assumed to be clustered at one end of the capillary,  $x = 0$ . Since the simulations represent experiments where the ends of the capillary are sealed with wax to prevent oxygen from entering the capillary, a zero flux condition was applied at the domain boundaries,  $x = 0, L$ . Thus the initial and boundary conditions becomes,

$$C_{O_2}(x, 0) = C_i, \frac{\partial C_{O_2}(0, t)}{\partial x} = 0, \frac{\partial C_{O_2}(L, t)}{\partial x} = 0 \quad (13)$$

In our simulation, we consider 1000 cells located at  $x = 0$  at  $t = 0$  that respond to an initially uniform concentration of oxygen and a fixed linear gradient of MeAsp in the capillary. Recall that MeAsp is only sensed but not metabolized by the bacteria, and therefore the MeAsp concentration remains constant in time. In the first time step, all cells were made to run (with run speed of  $U = 20 \mu\text{m}/\text{s}$ ) in the positive  $x$  direction for time duration,  $dt$ . At the new location, we solve the diffusion equation to update the concentration profile in the capillary. Next, the intracellular pathway equations are solved for all the cells to determine the probability of run or tumble for the next time step. In case of run, the cell is made to move a distance  $Udt$  at an angle chosen from a normal distribution with mean zero angle (about its previous angle) and a variance  $\sqrt{2D_r dt}$ . Here,  $D_r$  is the rotational diffusivity during the run mode (Vuppula et al., 2010). On the other hand, in case of a tumble event, the position of the cell is held constant and a new direction of the motion is chosen from a gamma distribution of turn angles with a mean turn angle of  $62^\circ \pm 1.1$  (Berg and Brown, 1972). Note that while the cell is allowed to move in the  $y$  direction, the net displacement along  $x$  is considered for determining the cell density. This is equivalent to applying a periodic boundary condition along  $y$ . The above steps are repeated at every time step to generate the cell density and oxygen concentration as function of the spatial coordinates. The average drift velocity of the cells was obtained by dividing the average position of the population by time.

### 3. RESULTS

#### 3.1 Excitation and adaptation

In a uniform environment *E. coli* exhibits a random motion and all its signaling proteins will be at steady state. For a step change in the attractant, the CheY-p concentration decreases immediately after which it slowly returns to its pre-stimulus steady state value. We simulate the dynamic response in terms of CheY-p concentration for step changes in MeAsp (Fig 1(A)) and oxygen (Fig 1(B)). While the drop in CheY-p concentration was immediate in both cases, the adaptation time for response to MeAsp was 100 times longer than that for oxygen. The parameters for the oxygen response mechanism were chosen so as to match the measured response reported by Yu et al. (2002) (Fig 2). The latter report their results in terms of the rate of change of direction per unit time (rcd in  $^\circ/\text{s}$ ) given by,

$$\text{rcd} = \frac{\sum_{i=1..m} |\Delta\theta_i|}{\sum_{i=1..m} \Delta t_i}$$

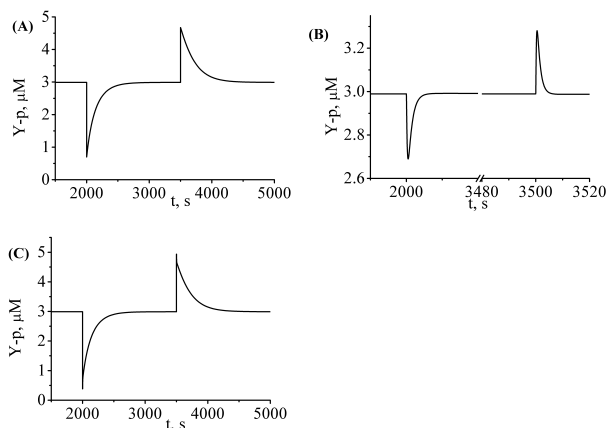


Fig. 1. Response of CheY-p protein in response to a step change in ligand concentration in A) MeAsp is changed from 10  $\mu\text{M}$  to 50  $\mu\text{M}$  at 2000 s and made it 10  $\mu\text{M}$  back at 3500 s and oxygen is maintained at 10  $\mu\text{M}$  B) Oxygen is changed from 10  $\mu\text{M}$  to 50  $\mu\text{M}$  at 2000 s and made it back to 10  $\mu\text{M}$  at 3500 s and MeAsp is maintained at 10  $\mu\text{M}$  C) Both Oxygen and MeAsp are changed from 10  $\mu\text{M}$  to 50  $\mu\text{M}$  at 2000 s and made it 10  $\mu\text{M}$  back at 3500 s

where  $\Delta\theta$  is the change in the angle between two time steps,  $m$  is the total number of time steps over a small time interval. There are six parameters to characterize the aerotaxis response (see equation (1) and (2)) which were fit using the aforementioned experimental results. Parameter values obtained are  $k_1 = 65.38$ ,  $\beta = 0.5$ ,  $k = 10$ ,  $k_o = 4.6 * 10^5 M$ ,  $n = 0.1$ ,  $\alpha = 0.35$  and  $\gamma = 0.65$ . It can be noted that after the parameter fitting, the model simulation captures the entire measured time profile of CheY-p. Successful prediction of experimental measurements supports our mathematical formulation as an effective way to describe the aerotaxis behavior of *E. coli*.

To study the combined response of the aerotaxis and chemotaxis pathways, simultaneous step changes in both oxygen and MeAsp were performed (Fig 1(C)). It is clear from the figure that the dip in the CheY-p concentration is higher than the individual response though the adaptation time is closer to that for MeAsp.

### 3.2 Response to linear gradient

Vuppula et al. (2010) have measured the drift velocity for a fixed linear gradient of MeAsp in a capillary. Here, cells were introduced at one end so that the cells travels up the gradient. During this process, the cells consume oxygen and set up a gradient of oxygen. Thus the measured drift velocity is the net chemotactic response to both the gradient of MeAsp and oxygen. The model equations were solved to obtain the drift velocity for various gradients of MeAsp with a fixed initial concentration of oxygen. Figure 4 compares the predicted drift velocity with measurements as a function of the distance from the plug ( $x = 0$ ) for different MeAsp gradients. The model was able to capture the decrease in the drift velocity away from the plug due to adaptation. Figure 4 shows that drift velocity at a distance of 2000 micron for varying gradients for MeAsp. While the

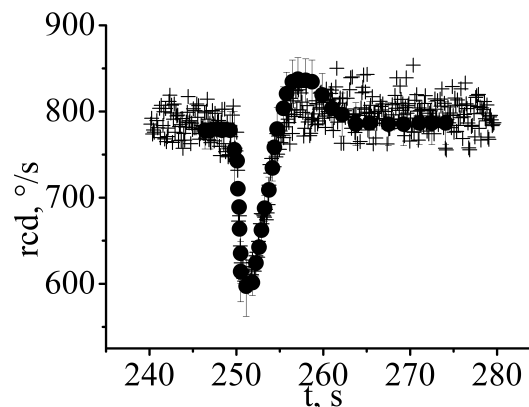


Fig. 2. *E. coli* response to step change from 0 to 0.0051 pmol in oxygen.  $\bullet$  is experimental measurements and  $+$  is model predictions. Band of values were obtained due to the stochastic behaviour in selecting angles

model is able to predict the observed trend, the predicted values are lower than the measurements.

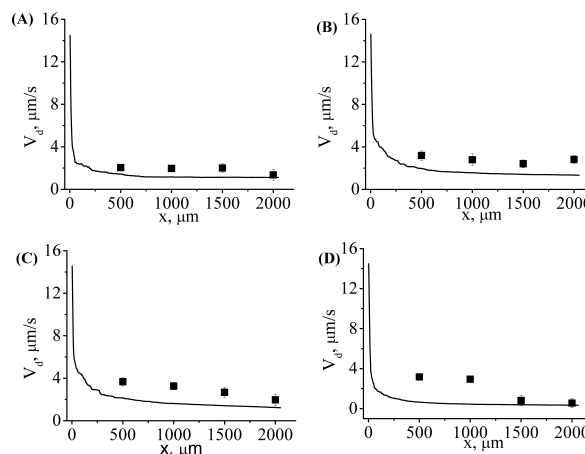


Fig. 3. Drift velocity as a function of position for four different gradients of MeAsp:  $\blacksquare$  is experimental measurements, thick line is model prediction. (A)  $G = 0.016 \mu\text{M}/\mu\text{m}$ ,  $L_0 = 16\mu\text{M}$  (B)  $G = 0.08 \mu\text{M}/\mu\text{m}$ ,  $L_0 = 80\mu\text{M}$  (C)  $G = 0.16 \mu\text{M}/\mu\text{m}$ ,  $L_0 = 160\mu\text{M}$  (D)  $G = 1.6\mu\text{M}/\mu\text{m}$ ,  $L_0 = 1600\mu\text{M}$ . In all the cases, the model predictions are close to the measurements

## 4. DISCUSSION

It is well known that bacteria consumes oxygen during the chemotactic response to a ligand. While most experiments and simulations focus on the latter, we attempt for the first time, to model the motion of bacteria in response to simultaneous variations in both oxygen and ligand concentration. The theoretical framework involves a detailed signaling pathway model for MeAsp and a phenomenological model for the response to oxygen. The model was able to simultaneously capture the consumption of oxygen along with its motion in response to the set gradient. Our model is able to qualitatively predict the motion of bacteria over a wide range of MeAsp gradients results though the predicted values are somewhat lower than

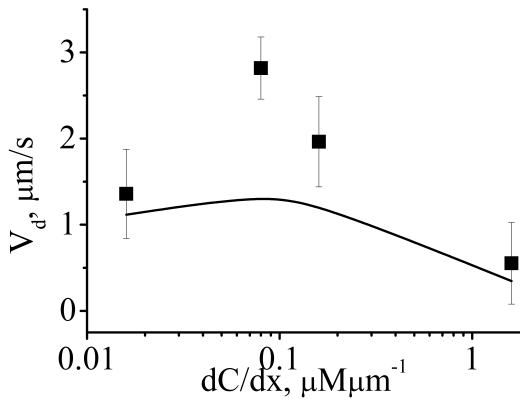


Fig. 4. Comparison of the measured drift velocity (■) with theoretical predictions at a distance of 2000μm from the plug for the K12 strain as a function of the MeAsp gradient. ■ is experimental measurements, thick line is model prediction.

the measurements. The discrepancy may be attributed to the absence of precise measurement of motor bias to step change in oxygen concentration over a wide range. However, the proposed model can be considered as a first step to model aerotaxis and further integrate chemotactic response to other ligands.

#### ACKNOWLEDGEMENTS

We thank Department of Science and Technology, India for providing financial assistance.

#### REFERENCES

- Barkai, N. and Leibler, S. (1997). Robustness in simple biochemical networks. *Nature*, 387, 913–917.
- Berg, H.C. and Brown, D.A. (1972). Chemotaxis in *Escherichia coli* analysed by three-dimensional tracking. *Nature*, 239, 502–507.
- Cussler, E.L. (1997). *Diffusion: Mass Transfer in Fluid Systems*. New York: Cambridge University Press.
- Eisenbach, M. (2004). *Chemotaxis*, chapter 3. Imperial college press.
- Emonet, T. and Cluzel, P. (2008). Relationship between cellular response and behavioral variability in bacterial chemotaxis. *Proc. Nat. Acad. Sci. USA*, 105, 3304–3309.
- Inoue, M. and Kaneko, K. (2006). Condition for intracellular adaptive dynamics for chemotaxis. *Phys. Rev. E*, 74, 011903.
- Laszlo, D.J. and Taylor, B.L. (1981). Aerotaxis in *Salmonella typhimurium*: Role of electron transport. *J Bacteriol*, 145, 990–1001.
- Li, M. and Hazelbauer, G.L. (2004). Cellular stoichiometry of the components of the chemotaxis signaling complex. *J Bacteriol*, 186, 3687–3694.
- Martin, D. (1932). The oxygen consumption of escherichia coli during the lag and logarithmic phases of growth. *J Gen Physiol.*, 15(6), 691708.
- Rebbapragada, A., Johnson, M.S., Harding, G.P., Zucarelli, A.J., Fletcher, H.M., Zhulin, I.B., and Taylor, B.L. (1997). The aer protein and the serine chemoreceptor tsr independently sense intracellular energy levels

and transduce oxygen, redox, and energy signals for *Escherichia coli* behavior. *Proc Natl Acad Sci U S A*, 94, 10541–10546.

Vuppula, R.V., Tirumkudulu, M.S., and Venkatesh, K.V. (2010). Mathematical modeling and experimental validation of chemotaxis under controlled gradients of methyl-aspartate in *Escherichia coli*. *Mol. BioSyst*, 6, 1082–1092.

Yu, H.S., Saw, J.H., Hou, S., Larsen, R.W., Watts, K.J., Johnson, M.S., Zimmer, M.A., Ordal, G.W., Taylor, B.L., and Alam, M. (2002). Aerotactic responses in bacteria to photoreleased oxygen. *FEMS Microbiol. Lett.*, 217, 237–242.

#### Appendix A. MODEL EQUATIONS FOR CHEMOSENSING

Let  $T_i$  represent the concentration of receptor complexes with  $i$  residues methylated and  $\alpha_i(L)$  denote the probability that the receptor complex  $T_i$  is active when the concentration of chemoattractant is  $L$ . The receptor complex can be in one of five methylation states with  $i = 0, 1, 2, 3$  or 4 methyl groups. The total concentration of active receptors is given by,

$$T^A = \sum_0^4 \alpha_i(L)T_i, \quad (\text{A.1})$$

while the total concentration of inactive receptors is given by,

$$T^I = \sum_0^4 (1 - \alpha_i(L))T_i. \quad (\text{A.2})$$

The binding kinetic equation for active receptor complex is given by,



The total active receptor complex concentration  $T_T^A$  is given by,

$$T_T^A \rightleftharpoons T_F^A + [T^A L] \quad (\text{A.4})$$

where  $T_F^A$  is free (non-ligand bound) active receptor complex concentration and  $[T^A L]$  is the ligand bound active receptor complex concentration respectively. The fraction of free active receptor complex concentration from the above equation is given by,

$$\frac{T_F^A}{T_T^A} = \frac{K_L}{K_L + L} \quad (\text{A.5})$$

where  $K_L$  is the ligand dissociation constant. Similarly, the fraction of ligand bound receptor complex concentration is given by,

$$\frac{[T^A L]}{T_T^A} = \frac{L}{K_L + L} \quad (\text{A.6})$$

The total probability of the receptor complex being in active state is the sum of the probabilities of the ligand bound and non ligand bound being in active state and is given by,

$$\alpha_i(L) = \frac{\alpha_i^L L}{K_L + L} + \frac{\alpha_i^0 K_L}{K_L + L} \quad (\text{A.7})$$

where the parameters assigned the following numerical values are,  $\alpha_0^L = 0$ ,  $\alpha_1^L = 0$ ,  $\alpha_2^L = 0.01$ ,  $\alpha_3^L = 0.05$ ,  $\alpha_4^L = 1$ ,  $\alpha_0^0 = 0$ ,  $\alpha_1^0 = 0.65$ ,  $\alpha_2^0 = 0.75$ ,  $\alpha_3^0 = 0.95$ ,  $\alpha_4^0 = 1$  and  $K_L = 250 \mu\text{M}$ . The Barkai and Leibler (Barkai and Leibler, 1997) model assumes that CheR ( $R$ ) binds to the inactive receptors ( $T^I$ ) and the phosphorylated CheB ( $B_p$ ) binds to the active receptors ( $T^A$ ). Assuming that, the methylation and demethylation reactions follows Michelis - Menten kinetics, the rate of demethylation and methylation is given by, respectively,

$$r_B = \frac{k_b(B_p)}{K_B + T^A} \quad (\text{A.8})$$

$$r_R = \frac{k_r(R)}{K_R + T^I} \quad (\text{A.9})$$

where,  $k_b = 0.208 \text{ s}^{-1}$  and  $k_r = 0.25 \text{ s}^{-1}$  are the rate constants and  $K_B = 0.54 \mu\text{M}$  and  $K_R = 0.39 \mu\text{M}$  are the Michaelis constants (Emonent and Cluzel, 2008) for receptor demethylation and methylation, respectively.

The rate of methylation is proportional to the concentration of inactive receptors  $(1-\alpha_i(L))T_i$ , and the rate of demethylation is proportional to the concentration of active receptors  $\alpha_i(L) T_i$ . For the receptor  $T_i$ , the rate of demethylation is  $r_B \alpha_i(L) T_i$  and the rate of methylation is  $r_R (1 - \alpha_i(L)) T_i$ , the mass balance equations for the corresponding receptor can be given by,

$$\frac{dT_0}{dt} = -r_R(1 - \alpha_0(L))T_0 + r_B\alpha_1(L)T_1 \quad (\text{A.10})$$

$$\begin{aligned} \frac{dT_1}{dt} = & -r_R(1 - \alpha_1(L))T_1 + r_B\alpha_2(L)T_2 \\ & + r_R(1 - \alpha_0(L))T_0 - r_B\alpha_1(L)T_1 \end{aligned} \quad (\text{A.11})$$

$$\begin{aligned} \frac{dT_2}{dt} = & -r_R(1 - \alpha_2(L))T_2 + r_B\alpha_3(L)T_3 \\ & + r_R(1 - \alpha_1(L))T_1 - r_B\alpha_2(L)T_2 \end{aligned} \quad (\text{A.12})$$

$$\begin{aligned} \frac{dT_3}{dt} = & -r_R(1 - \alpha_3(L))T_3 + r_B\alpha_4(L)T_4 \\ & + r_R(1 - \alpha_2(L))T_2 - r_B\alpha_3(L)T_3 \end{aligned} \quad (\text{A.13})$$

$$\frac{dT_4}{dt} = r_R(1 - \alpha_3(L))T_3 - r_B\alpha_4(L)T_4 \quad (\text{A.14})$$